A Composite TE-TFE-FE Model for Schottky Barrier Reverse Current over the Entire Electric-Field Range

Wenshen Li[1], Debdeep Jena[1,2,3], and Huili Grace Xing[1,2,3]
[1]School of Electrical and Computer Engineering, [2]Department of Materials Science and Engineering
[3]Kavli Institute at Cornell for Nanoscale Science, Cornell University, Ithaca, NY 14853, USA;
Email: wl552@cornell.edu / Phone: (412)500-1493

2022 Device Research Conference (DRC) | 978-1-6654-9883-8/22/$31.00 ©2022 IEEE | DOI: 10.1109/DRC55272.2022.9855788

Introduction:

Schottky barriers in wide bandgap (WBG) semiconductors can sustain very large electric fields under reverse bias due to the access of very large barrier heights (>1 eV) and the very high intrinsic breakdown field (>3 MV/cm) of WBG semiconductors [1]. Under high surface electric-fields (E), the ideal reverse-bias leakage current (J_R) is dominated by barrier tunneling rather than thermionic emission (TE), thus thermionic-field-emission (TFE) or field-emission (FE) becomes the dominant mechanism [1][2]. Therefore, to accurately describe the reverse current over the entire surface electric-field range, TFE and FE models are required in addition to the TE model.

We have recently developed a unified TE-TFE model that covers the entire TE and TFE regimes [3], however, the model is not applicable in the FE regime, the same goes for all other stand-alone TFE models. On the other hand, the well-known Murphy-Good FE model works well in the FE regime [2], but it is not applicable in the TFE regime. As a result, a gap exists in the TFE-to-FE transition region, as illustrated in **Fig. 1**, where no good analytical model exists. There has been an attempt to derive a unified TFE and FE model, however, the model is based on highly simplified emission integral with questionable accuracy, and image-force lowering is ignored [4]. In this context, we present a simple composite analytical model that covers the entire E-field range with excellent accuracy, with the use of an empirically-derived extrapolation function in the TFE-to-FE transition region.

Methods:

The integral for the barrier tunneling current under reverse bias is analytical intractable in the TFE-to-FE transition region [2]. To overcome this difficulty and knowing that the TE/TFE region and the FE region are well-described by the unified TE-TFE model [1] and Murphy-Good FE model [2][5], respectively (see **Fig. 1**), we seek to find an appropriate extrapolation function for the TFE-to-FE transition region. Based on the dominant exponential dependence of the TFE and FE models, it can be shown that leading term of $d(\sqrt{E}\ln J_\mathrm{R})/dE$ undergoes a transition from $E^{3/2}$ to $E^{-3/2}$ in the TFE-to-FE transition region, which means that $d(\sqrt{E}\ln J_\mathrm{R})/dE \sim E^0$ in the transition region. This has been confirmed empirically by numerical calculations, as shown in **Fig. 2a**. Thus, it is appropriate to adopt a linear relationship between $\sqrt{E}\ln J_\mathrm{R}$ and E in the transition region, where the current is defined as J_trans (**Fig. 3**). The linear coefficients therein are determined by two J_R values, J_1 and J_2, calculated at the upper E-limit of the unified TE-TFE model ($E_\mathrm{ulim,TFE}$) and at the lower E-limit of the Murphy-Good FE model ($E_\mathrm{llim,FE}$), respectively (see **Fig. 1b**). To ensure good accuracy of the extrapolation function for J_trans, the conditions for $E_\mathrm{ulim,TFE}$ and $E_\mathrm{llim,FE}$ have been modified with more strict requirements, as shown in **Fig. 4**. These modified conditions yield improved accuracy for J_1 and J_2, which in turn, enables a more accurate extrapolation function in the transition region.

Results and Discussion:

Comparisons between the composite TE-TFE-FE model relative to the reference numerical model [1] is shown in **Fig. 5**. The log error across the entire E-field range is within 2 dB (equivalent to a factor of 1.25) (**Fig. 2c**). The first derivative also shows very good agreement with the numerical model (**Fig. 2b**), indicating the extrapolation function for J_trans allows for a smooth transition between TFE and FE. We have used the composite model to analyze the reverse leakage characteristics in near-ideal 4H-SiC SBDs [6] and $\mathrm{Ga_2O_3}$ SBDs [1]. Very good agreement between experimental data and the composite model is observed across both the TE/TFE and the FE regimes, with the barrier height as the only fitting parameter (**Fig. 6**). Such an accurate analysis over the entire temperature and surface electric-field range is only possible with numerical calculations previously, as illustrated in **Table I**.

Conclusion: The composite TE-TFE-FE model successfully bridges the gap between the unified TE-TFE model and the Murphy-Good FE model with a simple empirical extrapolation function, allowing for accurate modeling of the Schottky barrier reverse current across the entire electric-field range. The closed-form and local nature of the composite model allows for easy implementation in TCAD tools for device design and analysis.

Acknowledgement: Supported under ULTRA (analytical modeling), an EFRC funded by the DOE (No. DE-SC0021230), AFOSR (No. FA9550-20-1-0148, numerical modeling), ComSenTer (experimental validation), one of the six SRC JUMP centers, and ACCESS ($\mathrm{Ga_2O_3}$ SBDs), an AFOSR Center of Excellence (No. FA9550-18-1-0529).

References: [1] W. Li et al., *Appl. Phys. Lett.* 116, 192101 (2020). [2] E. L. Murphy, and R. H. Good Jr., *Phys. Rev.* 102, 1464 (1956). [3] W. Li et al., *J. Appl. Phys.* 131, 015702 (2022). [4] S. Karmalkar et al., *Appl. Phys. Lett.* 82, 1431 (2003). [5] Li, W., 2020. Electrostatic engineering in wide-bandgap semiconductors for high power applications. [6] J. Nicholls et al., *Sci. Rep.* 9, 1 (2019).

978-1-6654-9883-8/22/$31.00 ©2022 IEEE

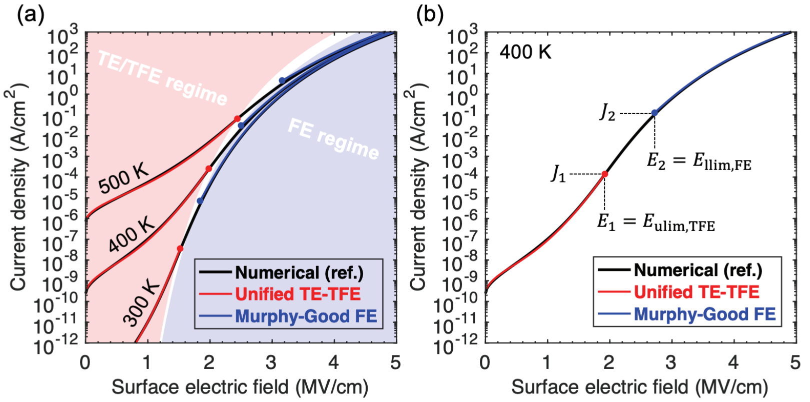

Fig. 1. (a) Illustration of the TE/TFE regime and the FE regime. Unified TE-TFE [3] and Murphy-Good FE [2] models both have limited applicable range. (b) Definition of J_1, J_2, E_1 and E_2 in the new composite model.

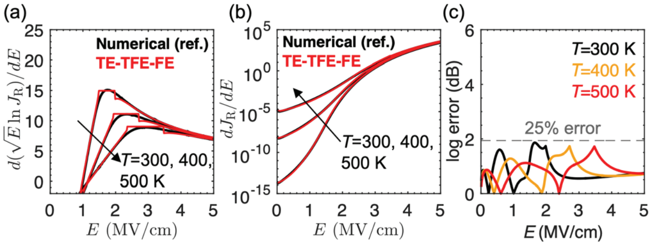

Fig. 2. First derivative of (a) $\sqrt{E}\ln J_{\mathrm{R}}$ and (b) J_{R}. The former shows $d(\sqrt{E}\ln J_{\mathrm{R}})/dE \sim E^0$ in the TFE-to-FE transition region, justifying the empirical form of J_{trans}. (c) Log error $|20\log_{10}(J_{\mathrm{R}}/J_{\mathrm{R,ref}})|$ relative to the numerical model ($J_{\mathrm{R,ref}}$). (ϕ_{B}=1.3 V, m^*=0.3 m_0, ε_{s}=10 ε_0).

Main equations

- $$J_{\mathrm{R}} = \begin{cases} J_{\mathrm{TFE}} + J_{\mathrm{TE}}, & \mathit{if}\ 0 < E \le E_{\mathrm{ulim,TFE}} \\ J_{\mathrm{trans}}, & \mathit{if}\ E_{\mathrm{ulim,TFE}} < E < E_{\mathrm{llim,FE}} \\ J_{\mathrm{FE}}, & \mathit{if}\ E \ge E_{\mathrm{llim,FE}} \end{cases}$$
- $J_{\mathrm{TFE}} + J_{\mathrm{TE}}$: unified TE-TFE model [3]
- J_{FE}: Murphy-Good FE model [2]
- Let $E_1 = E_{\mathrm{ulim,TFE}}$, $E_2 = E_{\mathrm{llim,FE}}$, $J_1 = \max(J_{\mathrm{TFE}} + J_{\mathrm{TE}})$, $J_2 = \min J_{\mathrm{FE}}$. Current in the TFE-to-FE transition region (J_{trans}) is given by
- $$\sqrt{E}\ln J_{\mathrm{trans}} = \frac{(E_2-E)\sqrt{E_1}\ln J_1 + (E-E_1)\sqrt{E_2}\ln J_2}{E_2-E_1}$$

Fig. 3. Main equations for the composite TE-TFE-FE model.

Modified conditions for $E_{\mathrm{ulim,TFE}}$ and $E_{\mathrm{llim,FE}}$

- Eq. 10 in Ref. 3 for $E_{\mathrm{ulim,TFE}}$
- $$\left(\frac{1+\sqrt{1-3ab}}{3b}\right)^2 + \left(\frac{3b}{2}t_{\mathrm{F}}^{\frac{1}{2}} + \frac{a}{2}t_{\mathrm{F}}^{-\frac{1}{2}} - 1\right)^{-1} < t_{\mathrm{F}} - \alpha_1$$
- α_1 is increased from 1 to 4 for improved accuracy.
- Eq. 58 in Ref. 2 for $E_{\mathrm{llim,FE}}$
- $$1 - \frac{ck_{\mathrm{B}}T}{\mathcal{E}_0} > (\alpha_2 f)^{\frac{1}{2}} \cdot \frac{k_{\mathrm{B}}T}{\mathcal{E}_0}$$
- α_2 is increased from 2 to 6 for improved accuracy. $\mathcal{E}_0 = \frac{m^* e^4}{(4\pi\varepsilon_{\mathrm{s}})^2\hbar^2}$ is the Bohr-energy constant.

Fig. 4. Modified conditions for $E_{\mathrm{ulim,TFE}}$ and $E_{\mathrm{llim,FE}}$ in the composite model with improved accuracy.

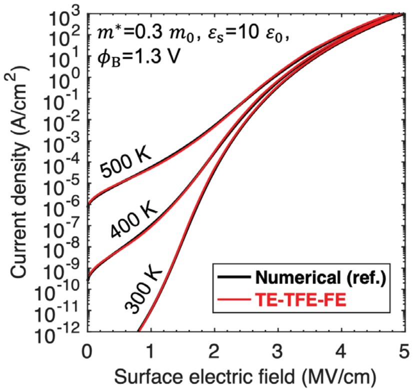

Fig. 5. The composite model exhibits excellent agreement against the reference numerical model [1].

TABLE I. Comparison of different models applicable at the FE regime.

	F-N tunneling	Murphy-Good FE [2]	Unified TFE-FE [4]	Numerical model [1]	**This work**
Temperature dependence	No	Yes	Yes	Yes	**Yes**
Image-force lowering	Yes	Yes	No	Yes	**Yes**
Entire *E*-field range	Yes	No	Yes	Yes	**Yes**
Closed-form expression	Yes	Yes	Yes	No	**Yes**
Doping effect*	No	No	No	Yes	**No**

*Insignificant below ~1×10^{18} cm^{-3}

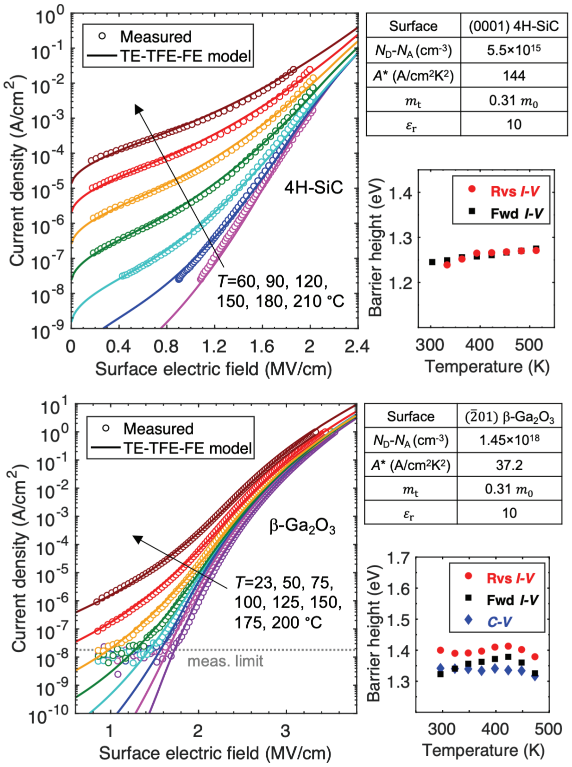

Surface	(0001) 4H-SiC
N_{D}-N_{A} (cm^{-3})	5.5×10^{15}
A^* (A/cm^{2}K^2)	144
m_{t}	0.31 m_0
ε_{r}	10

Surface	($\bar{2}$01) β-Ga$_2$O$_3$
N_{D}-N_{A} (cm^{-3})	1.45×10^{18}
A^* (A/cm^{2}K^2)	37.2
m_{t}	0.31 m_0
ε_{r}	10

Fig. 6. Analysis of near-ideal reverse leakage characteristics in (a) 4H-SiC SBDs [6] and (b) β-Ga$_2$O$_3$ SBDs [1] using the composite model, *with the barrier height as the only fitting parameter.*

978-1-6654-9883-8/22/$31.00 ©2022 IEEE